ARTHROPOD SYSTEMATICS & PHYLOGENY

77 (2): 251 – 265
2019

SENCKENBERG

Independent morphological and genetic diversification in close geographic and phylogenetic proximity: *Typoderus* weevils (Coleoptera) in the Uluguru Mountains, Tanzania

Vasily V. Grebennikov

Canadian Food Inspection Agency, 960 Carling Ave., Ottawa, ON, K1A 0C6, Canada [vasily.grebennikov@canada.ca]

Accepted on April 10, 2019.
Published online at www.senckenberg.de/arthropod-systematics on September 17, 2019.
Published in print on September 27, 2019.
Editors in charge: Sergio Pérez-González & Klaus-Dieter Klass.

Abstract. The Eastern Arc Mountains (EAM) of Tanzania form an island-type archipelago of wet and cool rainforests widely separated by extremely hot and dry savannah. This paper reports novel phylogeographical analyses of the low-dispersing and forest-dependent *Typoderus* weevils in the Uluguru block of the EAM. One mitochondrial and two nuclear loci were used to infer phylogenetic relationships among 70 *Typoderus* specimens, 52 of them from 22 geographically diversified Uluguru litter sifting samples. Various analyses consistently detected 11 geographically coherent *Typoderus* clades, six of them formed by the Uluguru specimens, where five are taxonomically interpreted as species: *T. admetus* sp.n., *T. furcatus*, *T. peleus* sp.n., *T. polyphemus* sp.n. and *T. subfurcatus*. The sixth Uluguru clade temporary named *Typoderus* sp. 1808 and consistently recovered with the different genetic markers comprises specimens morphologically similar to, and likely conspecific with, those of *T. admetus* sp.n. If so, then within the confined area of Uluguru forest (40 × 6 km) *T. admetus* sp.n. displays (i) high genetic differentiation without morphological change and (ii) high morphological variation with very little molecular differences; the driving factors of this phenomenon remain unknown. Observed distribution of *Typoderus* is interpreted as simple vicariance of a widespread ancestor; no evidence suggests a founder-based dispersal. This study rejects two widely assumed hypotheses that low dispersal (= flightless) forest-dependent clades are represented in each EAM block by an endemic species and that each such species within a single EAM block is panmictic.

Key words. Eastern Arc Mountains, DNA barcode, ITS2, 28S, sky islands.

1. Introduction

Assessment of the spatial and temporal components of evolution benefits from using geographical settings possessing discrete and contrasting abiotic characteristics. The Eastern Arc Mountains (EAM) of Tanzania (Fig. 1A,B), together with the nearby volcanic and lowland forests, is a well-publicized example of such sites. These highlands form an island-type archipelago of discrete blocks of wet and cool rainforests of different genesis and age, widely separated by extremely hot and dry savannah (Fig. 1B,D,E). The EAM forests are notable for supporting disproportionately high diversity of single-block endemics (Lovett & Wasser 1993). This phenomenon is linked to the relatively great age and high abiotic stability of EAM during the Plio- and Pleistocene climatic fluctuations, when the Afrotropical wet forest repeatedly and dramatically shrank to a few small core survival zones averaging about 10% of the present-day forest size (Hamilton & Taylor 1991; Maley 1996; deMenocal 2004). The EAM highlands, however, are thought to have retained their forest cover continuously since at least the Miocene, owing this stability to the reliable supply of atmospheric moisture coming from the nearby Indian Ocean and uninterrupted even during the most severe and repeated continental droughts corresponding to the glacial periods of the temperate zones (Lovett & Wasser 1993). This fundamental hypothesis underlying the observed biotic uniqueness of EAM was directly supported by the analyses of pollen, charcoal and carbon isotopes from deep soil probes taken in Udzungwa (Mumbi et al. 2008) and Uluguru (Finch et al. 2009), which revealed stable forest cover for the past 48,000 years, a period greatly exceeding the Last Glacial Maximum with its peak about 25,000 years ago.

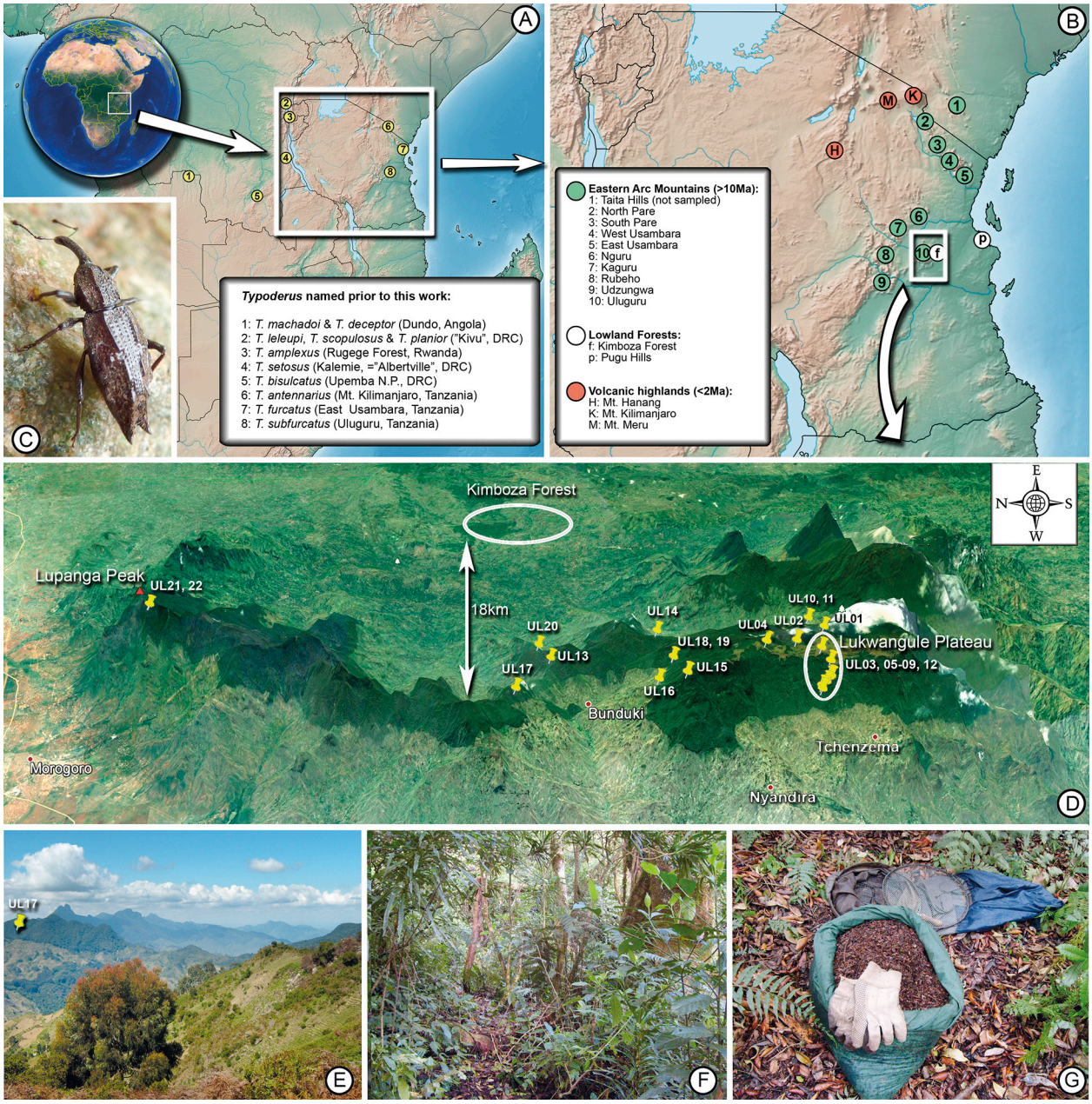

Fig. 1. A: Map showing the type localities of all 11 *Typoderus* species named prior to the present work. **B**: Map of sampled Tanzanian Eastern Arc Mountains and nearby forests with the Uluguru Mountains forming the focus of this study, map prepared with online software SimpleMappr (Shorthouse 2010). **C**: *Typoderus admetus* sp.n. **D**: Detailed map of the Uluguru Mountains showing positions of 22 litter sifting samples. **E**: View across the Bunduki gap, a human-made deforested corridor cutting through the narrow part of Uluguru forest, image taken northwards from UL18 sampling site. **F**: Sampling locality UL19 with numerous *Typoderus* weevils hidden in the forest floor. **G**: Litter sifting sample UL19 with the < 5mm litter fraction, and with sifter and finer insert mesh insert seen nearby.

Lovett & Wasser (1993) highlighted the exceptionally high and geographically structured biodiversity of EAM and triggered a plethora of phylogeographical studies (443 hits on Google Scholar for "Eastern Arc Mountains" and "phylogeography" queried on September 7, 2018). The great majority of these studies report that the low dispersal (= flightless) forest-dependent animal clades are often represented in each EAM block by an endemic species (e.g., Grebennikov 2017), which emerges as a general biodiversity pattern. Much of EAM-focussed research is biased towards taxonomically better known tetrapods, while the hyper-abundant invertebrates, including arthropods, is underrepresented, probably due to inadequate taxonomy (Grebennikov 2015a). Moreover, due to practical difficulties of accessing these steep and often far-away forests, published reports tend to prefer sampling of a larger number of EAM blocks with a smaller sample size, over thorough and multiple sampling of the same block. Such a data-gathering strategy underestimates single block inter- and intra-specific diversity by making an oversimplified assumption of the panmictic nature of the inhabitants of the single block. Only a few publications deviate from this sampling pattern by focussing on single block diversity (e.g., *Kinyon-*

gia boehmei (Lutzmann & Necas, 2002) chameleon in Taita Hills, Kenya: Measey & Tolley 2011), revealing complex spatial and temporal structures.

The present paper attempts to address both aforementioned shortcomings. For this purpose the Uluguru Mountains (Fig. 1B,D), which form the geographical focus of the present study, were exhaustively sampled for weevils of the genus *Typoderus* Marshall, 1953 (Fig. 1C). These relatively large and flightless beetles are obligate inhabitants of the wet and cool leaf litter of Afrotropical forest (Fig. 1A,F), and are never found outside (Fig. 1E) of its protective cover. Their phylogeographical potential was first recognized when numerous and externally variable adults were abundantly detected when sifting forest litter in Uluguru and other forests (Fig. 1B), some of them parts of EAM. Unlike many other nominal genera of Afrotropical weevils, *Typoderus* is likely monophyletic and its sister-group, the sympatric genus *Lupangus* Grebennikov, 2017, is reliably known (Grebennikov 2017). Owing to such a favourable combination of important characteristics, *Typoderus* weevils might be a promising tool for phylogeographical studies of EAM and comparable in this respect to other model flightless weevil clades, such as the Australasian-Oriental genus *Trigonopterus* Fauvel, 1862 (Toussaint et al. 2017), the predominantly Macaronesian genus *Laparocerus* Schoenherr, 1834 (Faria et al. 2016), or the *Exophthalmus* complex distributed through the Caribbean archipelago and Neotropical mainland (Zhang et al. 2017).

Advantageously, *Typoderus* does not contain many old obscure species names which might require study of types and perhaps re-sampling conspecific DNA-grade specimens in the type locality. Only five papers cover the entire history of *Typoderus* research and contain nearly all what is publicly known about these beetles: Marshall (1953) established the genus for two new species, *T. machadoi* Marshall, 1953 and *T. deceptor* Marshall, 1953, from northeastern Angola (Fig. 1A). Marshall (1955) added another species, *T. amplexus* Marshall, 1955, from Rugege forest in Rwanda (Fig. 1A). Later he (Marshall 1957) revised the genus and provided a key to eight species, five of them newly described: *T. furcatus* Marshall, 1957 from Amani in Tanzanian East Usambara and four species from the former Kivu province of Democratic Republic of the Congo (DRC): *T. leleupi* Marshall, 1957, *T. scopulosus* Marshall, 1957, *T. setosus* Marshall, 1957 and *T. planior* Marshall, 1957 (Fig. 1A). Voss (1962), when treating weevils of Upemba National Park in southeastern DRC, described *T. bisulcatus* Voss, 1962 (Fig. 1A). Finally, Voss (1965) described *T. antennarius* Voss, 1965 and *T. subfurcatus* Voss, 1965 from Tanzania (Mt. Kilimanjaro and Uluguru, respectively) (Fig. 1A). In the same work Voss (1965) proposed the subgenus *Entypoderus* for species with funicle consisting of seven antennomeres (type species: *T. deceptor*), while the nominative subgenus embraced the only two species with five antennomeres of the funicle (*T. machadoi*, the type species, and *T. antennarius*). Voss (1965) also singled out this genus as the sole member of the new subtribe Typoderina currently treated as a tribe and comprising about a dozen poorly known nominal genera (Lyal 2014; Grebennikov 2018a; not recovered as a clade in Grebennikov 2014a, 2017, 2018b). The genus *Typoderus* currently contains the 11 valid species-group names listed above, based on the type specimens from four sub-Saharan countries (Fig. 1A), housed in two European museums. No novel data of these species have been ever reported in publications other than the original descriptions. After this short period of activity (1953–1965), the genus has ceased to attract attention and no detailed biological, phylogenetic and DNA information has been published since except for a recent use of three nominal Tanzanian species as outgroup taxa (Grebennikov 2014a,b, 2017).

The purpose of this paper is to test two hypotheses often implicitly assumed in the majority of EAM studies: i) that low dispersal (= flightless) forest-dependent clades are represented in each EAM block by an endemic species and ii) that each such species within a single EAM block is panmictic. To achieve this, the following four specific goals of this work are: (1) to thoroughly document morphological and genetic diversity of *Typoderus* beetles in Uluguru; (2) to generate a DNA-based phylogenetic hypothesis of Uluguru *Typoderus* within the broader geographical and phylogenetic framework of this genus; (3) to provide spatial and temporal interpretation of the detected phylogeographic structure specifically targeting diversification and dispersal events in the context of the Pliocene–Pleistocene climatic fluctuations and (4) to update *Typoderus* taxonomy by elucidating existing and generating new Linnaean names for morphologically diagnosable *Typoderus* clades worthy of formal species status. Last but not least, the genus *Typoderus* will itself be tested as a promising source of phylogeographical data.

2. Material and methods

2.1. Geographic focus

Three factors influenced the choice of the Uluguru Mountains. Firstly, their closed-canopy wet rainforest of about 40 km in length and 6 km in width (Fig. 1D) is among the largest and best preserved EAM forest blocks. Secondly, relative ease of access from various points (Fig. 1D) renders the Uluguru forest suitable for geographically diversified sampling. Thirdly, preliminary fieldwork in 2002 indicated that *Typoderus* weevils are abundant in Uluguru and are likely represented by more than a single species known from there so far (*T. subfurcatus*).

2.2. Specimen sampling and handling

A total of 22 sifting samples were taken in Uluguru (sample codes UL01 to UL22, Fig. 1D; full label data in Ta-

Table 1. GenBank accession numbers of *Typoderus* weevils and a single non-*Typoderus* outgroup taxon; for sample code see Table S1.

Voucher	Species	Highland	Sample	COI	ITS2	28S
CNCCOLVG00001764	*T. admetus* sp.n.	Uluguru	UL01	JN282467	KY110466	KY110664
CNCCOLVG00001765	*T. admetus* sp.n.	Uluguru	UL01	JN282468	KY110444	KY110641
CNCCOLVG00001766	*T. subfurcatus*	Uluguru	UL01	JN282469	KY110473	KY110671
CNCCOLVG00001808	*Typoderus* sp. 1808	Uluguru	UL03	JN282483	KY110451	KY110649
CNCCOLVG00001809	*T. admetus* sp.n.	Uluguru	UL03	JN282484	none	KY110643
CNCCOLVG00001811	*T. admetus* sp.n.	Uluguru	UL03	JN282486	KY110469	KY110667
CNCCOLVG00001824	*T. subfurcatus*	Uluguru	UL03	JN282495	KY110480	KY110679
CNCCOLVG00001865	*T. admetus* sp.n.	Uluguru	UL03	JN282502	KY110470	KY110668
CNCCOLVG00001867	*T. admetus* sp.n.	Uluguru	UL03	JN282504	KY110454	KY110652
CNCCOLVG00002048	*T. admetus* sp.n.	Uluguru	UL10	KY034337	KY110456	KY110654
CNCCOLVG00002050	*T. admetus* sp.n.	Uluguru	UL10	KY034319	KY110440	KY110637
CNCCOLVG00002051	*T. admetus* sp.n.	Uluguru	UL10	KY034327	KY110448	KY110646
CNCCOLVG00002058	*T. admetus* sp.n.	Uluguru	UL11	KY034342	KY110460	KY110658
CNCCOLVG00002059	*Typoderus* sp. 1808	Uluguru	UL11	KY034350	KY110472	KY110670
CNCCOLVG00002060	*T. admetus* sp.n.	Uluguru	UL11	KY034326	KY110447	KY110645
CNCCOLVG00002062	*T. admetus* sp.n.	Uluguru	UL11	KY034365	KY110485	KY110684
CNCCOLVG00002063	*T. admetus* sp.n.	Uluguru	UL11	KY034311	KY110436	KY110633
CNCCOLVG00002064	*T. admetus* sp.n.	Uluguru	UL11	KY034303	KY110430	KY110626
CNCCOLVG00002065	*T. subfurcatus*	Uluguru	UL11	KY034325	KY110446	KY110644
CNCCOLVG00002070	*T. admetus* sp.n.	Uluguru	UL13	KY034301	KY110429	KY110625
CNCCOLVG00002073	*T. admetus* sp.n.	Uluguru	UL13	KY034338	KY110458	KY110656
CNCCOLVG00002075	*T. subfurcatus*	Uluguru	UL13	KY034304	KY110432	KY110628
CNCCOLVG00002086	*Typoderus* sp. 1808	Uluguru	UL15	KY034359	KY110479	KY110677
CNCCOLVG00002087	*T. subfurcatus*	Uluguru	UL15	KY034328	KY110450	KY110648
CNCCOLVG00002088	*T. subfurcatus*	Uluguru	UL15	KY034307	KY110434	KY110630
CNCCOLVG00002103	*T. admetus* sp.n.	Uluguru	UL16	KY034309	KY110435	KY110632
CNCCOLVG00002105	*T. admetus* sp.n.	Uluguru	UL16	KY034364	KY110484	KY110683
CNCCOLVG00002111	*Typoderus* sp. 1808	Uluguru	UL17	KY034357	KY110476	KY110674
CNCCOLVG00002117	*T. peleus* sp.n.	Uluguru	UL17	KY034322	KY110442	KY110639
CNCCOLVG00002118	*T. peleus* sp.n.	Uluguru	UL17	KY034300	KY110427	KY110624
CNCCOLVG00002121	*Typoderus* sp. 1808	Uluguru	UL17	KY034297	KY110426	KY110623
CNCCOLVG00002124	*T. admetus* sp.n.	Uluguru	UL17	KY034308	none	KY110631
CNCCOLVG00002130	*T. peleus* sp.n.	Uluguru	UL17	KY034348	KY110471	KY110669
CNCCOLVG00002132	*T. admetus* sp.n.	Uluguru	UL17	KY034356	KY110474	KY110672
CNCCOLVG00002133	*T. polyphemus* sp.n.	Uluguru	UL17	KY034361	KY110482	KY110681
CNCCOLVG00002134	*T. polyphemus* sp.n.	Uluguru	UL17	KY034347	KY110468	KY110666
CNCCOLVG00002135	*T. admetus* sp.n.	Uluguru	UL17	KY034323	KY110443	KY110640
CNCCOLVG00002151	*T. admetus* sp.n.	Uluguru	UL18	KY034333	KY110452	KY110650
CNCCOLVG00002154	*Typoderus* sp. 1808	Uluguru	UL19	KY034317	KY110438	KY110635
CNCCOLVG00002155	*T. admetus* sp.n.	Uluguru	UL19	KY034292	KY110422	KY110620
CNCCOLVG00002159	*T. subfurcatus*	Uluguru	UL20	KY034294	KY110423	KY110621
CNCCOLVG00002160	*T. subfurcatus*	Uluguru	UL20	KY034296	KY110425	KY110622
CNCCOLVG00002171	*T. admetus* sp.n.	Uluguru	UL20	KY034313	KY110437	KY110634
CNCCOLVG00002174	*T. furcatus*	Uluguru	UL20	KY034360	KY110481	KY110680
CNCCOLVG00002175	*T. polyphemus* sp.n.	Uluguru	UL20	KY034363	KY110483	KY110682
CNCCOLVG00002176	*T. furcatus*	Uluguru	UL20	KY034336	KY110455	KY110653
CNCCOLVG00002177	*T. furcatus*	Uluguru	UL20	KY034358	KY110478	KY110676
CNCCOLVG00003019	*T. furcatus*	East Usambara	EU03	KJ445682	KY250483	KY250478
CNCCOLVG00003020	*T. furcatus*	East Usambara	EU03	KJ445697	KY110461	KY110659
CNCCOLVG00003060	*Lupangus asterius*	East Usambara	EU05	KY034280	KY250485	KY250480
CNCCOLVG00003064	*T. furcatus*	East Usambara	EU05	KJ445710	KY110475	KY110673
CNCCOLVG00003094	*T. furcatus*	East Usambara	EU08	KJ445694	KY110449	KY110647
CNCCOLVG00003606	*T. peleus* sp.n.	Kimboza forest	KM02	KY110593	KY110431	KY110627
CNCCOLVG00003611	*T. subfurcatus*	Kimboza forest	KM02	KY110602	KY110477	KY110675
CNCCOLVG00003620	*T. peleus* sp.n.	Kimboza forest	KM03	KY110592	KY110428	none
CNCCOLVG00003621	*T. peleus* sp.n.	Kimboza forest	KM03	KY110591	KY110424	none
CNCCOLVG00003622	*T. subfurcatus*	Kimboza forest	KM03	KY110599	KY110464	KY110662
CNCCOLVG00003632	*Typoderus* sp. 1808	Uluguru	UL20	KY034306	KY110433	KY110629
CNCCOLVG00003633	*T. admetus* sp.n.	Uluguru	UL20	KY034321	KY110441	KY110638
CNCCOLVG00003634	*T. admetus* sp.n.	Uluguru	UL21	KY034341	KY110459	KY110657
CNCCOLVG00003638	*T. subfurcatus*	Uluguru	UL21	KY034353	KY250486	KY250481
CNCCOLVG00005460	*T. peleus* sp.n.	Pugu Hills	PG01	KY110603	none	KY110678
CNCCOLVG00005461	*T. peleus* sp.n.	Pugu Hills	PG01	KY110597	KY110462	KY110660
CNCCOLVG00005462	*T. peleus* sp.n.	Pugu Hills	PG01	KY110601	KY110467	KY110665
CNCCOLVG00007164	*T. antennarius*	Mt Kilimanjaro	KL07	KY110595	KY110453	KY110651
CNCCOLVG00007166	*T. antennarius*	Mt Kilimanjaro	KL07	KY250487	KY250484	KY250479
CNCCOLVG00007167	*T. antennarius*	Mt Kilimanjaro	KL07	KY110596	KY110457	KY110655
CNCCOLVG00007169	*T. antennarius*	Mt Kilimanjaro	KL07	KY110598	KY110463	KY110661
CNCCOLVG00007173	*T. subfurcatus*	Kimboza forest	KM03	KY110594	KY110445	KY110642
CNCCOLVG00007175	*T. subfurcatus*	Kimboza forest	KM03	KY110600	KY110465	KY110663
CNCCOLVG00007253	*T. admetus* sp.n.	Uluguru	UL13	KY034318	KY110439	KY110636

ble S1) targeting predominantly easier-to-access central and southern parts, in the vicinity of Bunduki village and around the Lukwangule plateau, respectively (Fig. 1D). Fieldwork was conducted during the rainy seasons when *Typoderus* adult are abundantly sampled by sifting forest leaf and twig litter (Fig. 1G) with a hand-held sifter, followed by an overnight in-doors specimen extraction in suspended Winkler funnels (Grebennikov 2017). Specimens were preserved in 96% ethanol, which was replaced in the field at least twice within intervals of 2–5 days, to maintain its high concentration. All herein reported specimens have a label with the code CNC COLVG0000XXXX; the last four Xs serve as unique identifiers (Table 1, Fig. 2). All studied specimens are adults, except for one larva (specimen 2004) and one pupa (specimen 2045, Figs. S1, S2). All newly sampled specimens, including the holotypes of three newly described species, are deposited in the Canadian National Collection of Insects, Arachnids and Nematodes in Ottawa, Canada (CNC).

2.3. Specimen selection for DNA barcoding followed by Neighbour Joining (NJ) and Barcode Index Number (BIN) clustering

About one thousand *Typoderus* specimens from Uluguru were initially assessed under a dissecting microscope for their morphological variation. No sorting into morphospecies took place prior to DNA analysis (or, rather, was impossible due to extremely variable morphology not rendering itself for easy species delimitation, see Discussion); instead the morphologically most dissimilar specimens were subjectively selected for DNA barcoding (= sequencing of 658 bp of COI-5', Hebert et al. 2003a,b). All laboratory work (DNA extraction, purification, PCR and bidirectional sequencing) was performed in the "Canadian Center for DNA Barcode" (CCDB, http://www.ccdb.ca/) at the University of Guelph, Ontario, Canada, following the standard laboratory protocol (Ivanova et al. 2006). A cocktail of two primer pairs was used to amplify the DNA barcoding fragment (Table S2). A total of 105 *Typoderus* from Uluguru were successfully DNA barcoded (Figs. S1, S2); their sequences, electropherograms, gel images, specimen data and specimen images (Fig. S2) can be seen in the public Barcode of Life Data System (BOLD, Ratnasingham & Hebert 2007) dataset DS-TYPODUL1 available online at dx.doi.org/10.5883/DS-TYPODUL1. Alignment of these sequences was trivial and contained no insertions/deletions (= indels). Topological clustering of these 105 terminals was done using the online BOLD tree-building engine utilizing the NJ algorithm, while clustering in BINs was done automatically by BOLD following the algorithm described by Ratnasingham & Hebert (2013).

Table 2. DNA fragments used in analyses.

Fragment	#	min	max	aligned	positions	model
COI-5P	71	589	658	658	1 to 658	GTR+G+I
ITS2	68	214	585	768	659 to 1380	K2+G
28S	69	219	571	595	1381 to 1975	K2+G

2.4. Three-marker matrix formation

Selection of a subset of Uluguru *Typoderus* specimens to be sequenced for two additional nuclear DNA markers, ITS2 and 28S (both fragments located 268 bp apart when compared to the *Papilio xuthus* L., 1767 rRNA reference sequence AB674749.1; Futahashi et al. 2012), was based on the obtained NJ clustering topology (Fig. S2). The observed diversity of the DNA barcode was taken as a proxy to hypothesize diversity of the two other nuclear markers. Fifty-two adult-only terminals were selected to best represent clusters of Uluguru *Typoderus* recovered in the NJ analysis (Fig. S2). To place Uluguru specimens in a wider geographical and phylogenetic context, 18 non-Uluguru *Typoderus* terminals were added: four specimens of *T. antennarius* from Mt. Kilimanjaro, four specimens of *T. furcatus* from East Usambara, three and four specimens each representing a distinct morphospecies from the nearby Kimboza Forest (Fig. 1D) and three seemingly conspecific specimens from Pugu Hills (Fig. 1B). No DNA data of other named *Typoderus* were available. *Lupangus asterius* Grebennikov, 2017 from East Usambara, the type species of the genus sister to *Typoderus* (Grebennikov 2017), was added in the matrix to root the topology. The total number of terminals in the three-fragment dataset was 71 (Table 1); their sequences, electropherograms, gel images, specimen data and specimen images can be seen in the public BOLD dataset DS-TYPODUL2 available online at dx.doi.org/10.5883/DS-TYPODUL2.

Alignment of ITS2 and 28S sequences was made online using MAFFT 7 platform (Katoh et al. 2002; Katoh & Toh 2008a) with the Q-INS-i algorithm (Katoh & Toh 2008b) utilising the secondary structure information (Table 2). No parts of the alignments were excluded from the analyses. Three aligned single-fragment datasets were concatenated using Mesquite 3.11 (Maddison & Maddison 2011).

2.5. Four Maximum Likelihood (ML) analyses

Four ML phylogenetic analyses were performed, each utilizing a different dataset of either one of three individual fragments, or the concatenated matrix (Table 2). Single fragment analyses were conducted with ML phylogenetic method using MEGA7 (Kumar et al. 2016) first by identifying the best nucleotide substitution model using the highest BIC score (Table 2), followed by an analysis with 100 bootstrap (Felsenstein 1985) replicates. Analy-

sis of the concatenated dataset was conducted with M phylogenetic method using RAxML 7.2.7 (Stamatakis et al. 2008) algorithm on a computer cluster at the Cyberinfrastructure for Phylogenetic Research (CIPRES) (Miller et al. 2010) with 100 bootstrap replicates and data partitioned in three fragments (Table 2), each fragment forming an independent partition. Obtained topologies were visualized using FigTree v1.4 (Rambaut 2014).

2.6. Bayesian age estimation of mDNA lineage separations

Two temporal analyses were performed to estimate absolute time of divergence between mtDNA lineages of *Typoderus*. Due to uncertainty on the deeper splits (= events separating groups of species within the genus *Typoderus*), this analysis targeted mainly shallow evolutionary events (= those within nominal species, or separation between two sister species). For this purpose the DNA barcoding matrix of 71 terminals used for the ML analysis (Table 2) was reduced by exclusion of the only non-*Typoderus* terminal (*Lupangus asterius* Grebennikov, 2017) to minimize bias associated with long branches. The resulting 70-terminal matrix was analysed with Bayesian inference phylogenetic method using BEAST 1.8 (Drummond et al. 2012) with default priors to simultaneously estimate an ultrametric phylogenetic tree and ages of diversification. In the absence of time calibrating data, a uniform substitution rate of 0.018 nucleotide substitutions per site per million years per lineage (subs/s/Myr/l) was used, in agreement with results obtained for COI-5' in other beetles (Papadopoulou et al. 2010; Andújar et al. 2012). No clades were enforced prior to the analysis, and the root was placed automatically on the longest branch. The GTR+G evolutionary model identified earlier for this matrix (Table 2) was used and the MCMC chains ran for 10 million generations. Consensus trees were estimated with TreeAnnotator (Drummond et al. 2012) discarding the 25% initial trees as a burn-in fraction. Posterior probabilities were considered as a measure of node support. Second temporal analysis was performed using the same methods applied to the same matrix reduced to 22 terminals, where the basalmost split in each among 11 geographically coherent clades A–K (Fig. 2) was represented by a pair of terminals.

2.7. Specimen sexing and genitalia dissection

No attempt was made to consistently dissect all analysed specimens and to determine if any of the observed diversity correlates with the shape of male genitalia (or might perhaps be linked with sexual dimorphism, which is weak among most of Molytinae and was never recorded for Typoderini). Only male holotypes of three herein newly described species (Fig. 4) plus three male specimens representing sympatric Uluguru clades (Fig. 5) were dissected and their genitalia illustrated.

2.8. Matching Linnaean names and clades, description of new taxa

The type specimens of *T. furcatus* and *T. subfurcatus* described from the region were examined to corroborate their conspecificity with the newly sampled and genetically analysed topotypic specimens. Decision on species delimitation, either of those already named or of three newly named species, was done using the unified species concept (de Queiroz 2007) and the practical need for species names (Ward 2011). Following Grebennikov (2015b, 2017), morphological description of new species is presented using a numerical matrix linked to a list of diagnostic characters with contrasting states.

3. Results

3.1. Topology selection, BIN and species name matching

The ML tree from the concatenated 71-terminal matrix (Fig. 2) is selected as the reference topology to represent the phylogenetic signal detected in this study. Mainly congruent topologies obtained from five other analyses (three fragment-specific ML analyses and two temporal analyses using 70- and 22-terminal matrixes depicted on Figs. S3, S4, S5, S6 and Fig. 3, respectively) are used only for comparison. Concatenated analysis grouped *Typoderus* terminals in 11 geographically (and, in a lesser degree, morphologically; see Discussion) coherent clades (clades A–K in Fig. 2) with high bootstrap support (83–100%). Six of *Typoderus* clades (A, B, E, H, J, K) are formed by the Uluguru specimens. Three clades are formed by topotypical specimens of three nominal *Typoderus* species (*T. furcatus* from East Usambara, *T. antennarius* from Mt. Kilimanjaro and *T. subfurcatus* from Uluguru, clades C, D, J, respectively); those of *T. furcatus* and *T. subfurcatus* have respective sister-clades (clades B and I, Fig. 2) of morphologically similar and therefore potentially conspecific specimens (see Discussion). Sister-group relationships among these clades A–K were resolved with mainly medium- or high-support values (except two low values of 28% and 53%). The total of 32 BINs were identified for 70 *Typoderus* specimens forming 11 geographically coherent clades (Fig. 2), varying between one and eight BINs per clade.

3.2. Divergence dating

Temporal analyses of the 22-terminal *Typoderus*-only matrix (Fig. 3) recovered the same 11 geographically coherent clades as those depicted on the concatenated ML topology (Fig. 2), even though *Typoderus* sp. 1808 had a different sister-group. The most recent common ancestors of any of these 11 clades shared with the respective sister

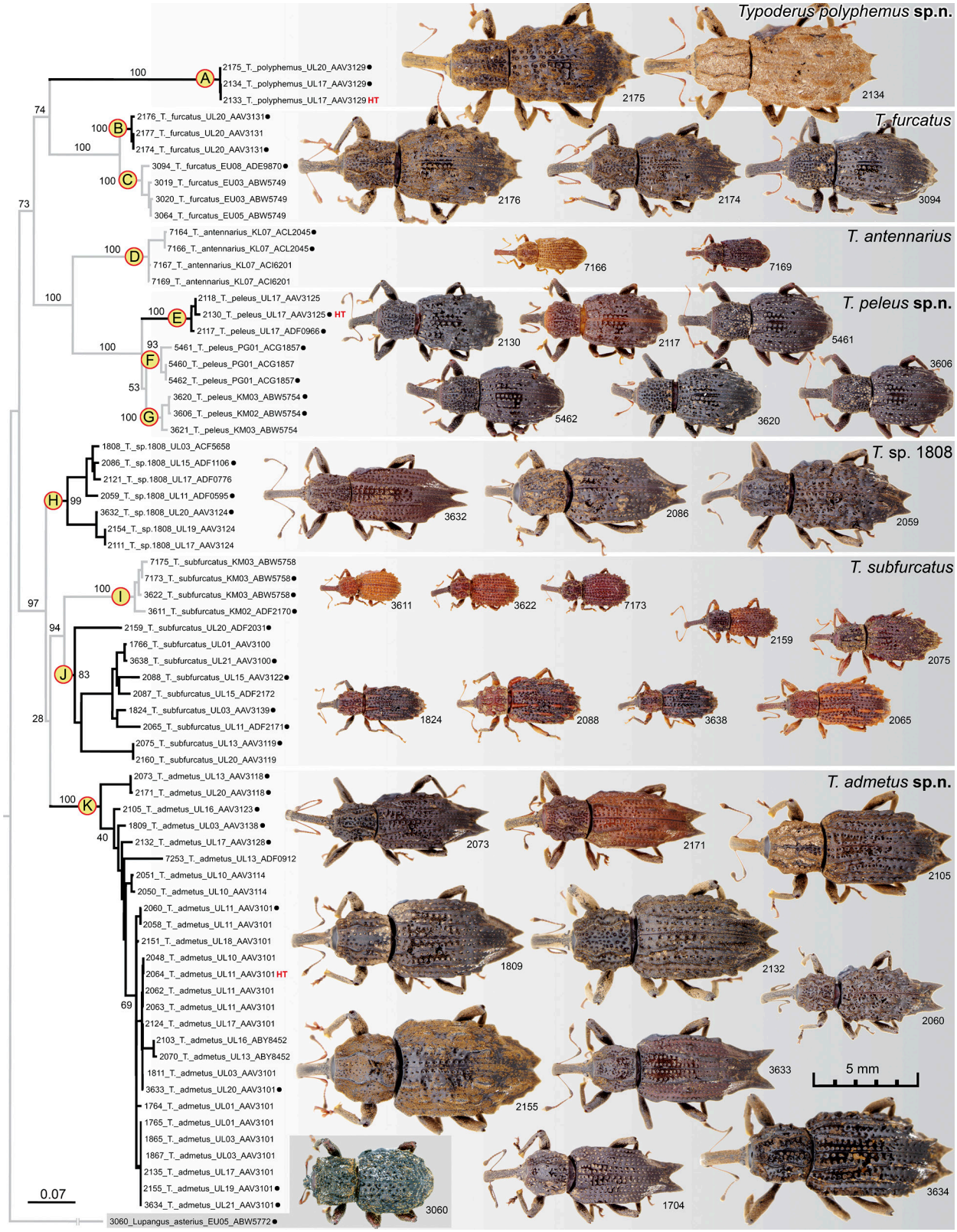

Fig. 2. Maximum Likelihood inference phylogram of Uluguru *Typoderus* weevils from the concatenated matrix of 2,025 bp. Eleven geographically coherent clades are labelled A–K; six of them from Uluguru are in black. Digits at internodes are bootstrap values. Terminal labels consist of a specimen number, taxonomic name, sample number and BIN. Black dots behind terminals indicate those illustrated; all images are to scale. Letters HT denote holotypes of three newly described species.

group were dates from 2.61 MYA and older, while the basal-most divergent events within these 11 clades started to occur from 9.4 MYA (Fig. 3). Similarly performed analysis of the 70-terminal *Typoderus*-only matrix produced a tree (Fig. S6) with the same branching pattern and comparably dated separation events.

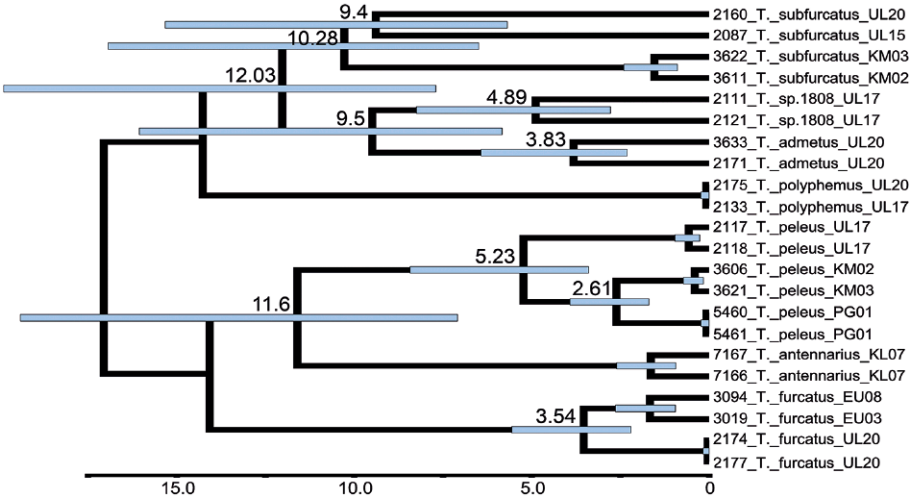

Fig. 3. Ultrametric time tree of 22 select *Typoderus* obtained with BEAST using 0.018 subs/s/Myr/l rates for COI-5‘. Terminal labels as in Fig. 4 (except that BINs are excluded). Numbers on scale and at nodes are million years before present. Node bars represent 95% confidence interval.

4. Discussion

4.1. Phylogenetic structure of analysed *Typoderus* and logic of species delineation

Since 46 among 70 herein analysed *Typoderus* specimens likely represent yet unnamed species, the first practical need is to formally describe the new species and, therefore, to integrate the obtained results in the framework of the Linnaean taxonomy. The first step in this process is to test the utility of BINs as a proxy to delimit species boundaries. Calculation of BINs is linked to the pre-selected gap value, which is about 2.2% of the COI-5’ p-distance (the latter variously defined), above which threshold the BOLD algorithm tend to assign two DNA barcodes to different BINs (Ratnasingham & Hebert 2007). A number of studies agree that the BIN approach might indeed be adequate in suggesting a candidate species in clades of relatively highly volant and predominantly panmictic organisms (for example 3,565 species of North American owlet moth and their allies corresponded to 3,816 BINs; Zahiri et al. 2017). In clades of low-dispersal arthropods, such as Melanesian *Trigonopterus* weevils, pairwise uncorrected p-distance might exceed 10% (Tänzler et al. 2012), compromising universal utility of the BIN approach. Recovery of 32 BINs for 11 *Typoderus* clades suggest that the BIN approach can inflate the number of biological entities by exaggerating observed differences in the DNA barcode. Indeed, the morphologically similar specimens 7166 and 7169 of *T. antennarius* are assigned to different BINs (Fig. 2). These results suggest that the BIN approach should be taken with caution, particularly among low-dispersing organisms with presumably low gene flow.

How to match the 11 recovered clades and three existing nominal *Typoderus* species? Three clades (C, D and J, Fig. 2) are formed by specimens morphologically similar to the historical types and sampled in the respective type localities. This establishes their taxonomic identity as *T. furcatus*, *T. antennarius*, and *T. subfurcatus*, respectively. The remaining eight geographically coherent clades, of them five from Uluguru, need to be either taxonomically assigned to the existing names, or be newly named. Two of these clades (B and I) form sister groups to the named species (*T. furcatus* and *T. subfurcatus*, respectively) and, considering morphological similarities and relative geographic proximity, are best treated as conspecific with the latter. Contrastingly, the sister-group of *T. antennarius* consists of specimens most dissimilar to the latter, thus rejecting a hypothesis of the conspecificity. Considering that no other named *Typoderus* are known from Tanzania, all six unnamed clades (A, E, F, G, H, K) have, therefore, been assigned to newly described species. The only remaining question is how many new species have to be established?

Two new species are relatively easy to delimit: one of them is represented by the clade A from Uluguru, while another is the clade sister to *T. antennarius* and formed by clades E, F and G from Uluguru, Pugu Hills and Kimboza Forest (Fig. 2). In both cases candidate species reflect well the observed genetic and morphological clustering (Fig. 2). Taxonomic interpretation of the two remaining unnamed clades (H and K) is far from straightforward and likely forms the greatest challenge (and the greatest discovery) of this study.

4.2. Clades H and K: morphological diversification without genetic change and vice versa

To facilitate taxonomic interpretation of clades H and K (Fig. 2), three factors are to be considered. Firstly, these clades, together with *T. subfurcatus*, form a strongly supported (97%) clade restricted to Uluguru (except for the subclade I of *T. subfurcatus* from the nearby Kimboza Forest). Secondly, morphologically indistinguishable specimens from the same sample attributed to ei-

ther clade H or K (see, for example, specimens 3632 and 2171 from the sample UL20, Fig. 2) suggest significant genetic differentiation without corresponding morphological change ("non-adaptive radiation" or "cryptic species complexes", Barley et al. 2013). Thirdly, clade H and even more so clade K (the latter relatively abundantly represented in the analysis by 27 specimens) each includes specimens whose morphologically dissimilarity within each clade would normally reject an assumption of conspecificity (compare, for example, acutely dissimilar specimens 2060, 2073, 2132 and 2155 in clade K, Fig. 2); this result suggests significant morphological differentiation without corresponding genetic change ("adaptive radiation" or "great speciators", Barley et al. 2013). Each of these phenomena are frequently encountered (Barley et al. 2013 and references there), however they are normally spatially (Bray & Bocak 2016) and phylogenetically separated. Co-occurrence of both phenomena within the same shallow clade (or perhaps even within the same species, see below) restricted to a single and relatively small forest makes, therefore, the reported *Typoderus* results spectacular.

Indeed, the morphological diversity observed in clade K (and, to a lesser, extend, in clade H) is remarkable and intimately linked with the design of this study. Original attempts to sort the encountered Uluguru *Typoderus* into morphospecies, either in the field or when sorting them in the lab, were abandoned due to difficulties in identifying distinct groups of morphologically coherent specimens. It was possible, however, to quickly detect two main entities: the smaller and reddish species (= *T. subfurcatus*) and the rest of Uluguru *Typoderus* represented by notably larger and darker specimens (clades A, B, E, H and K). Morphological distinctness of clade A (such as the greatest body size) eroded with detection of comparably large specimens of the clade B (for example 2176, Fig. 2). Another field-suspected candidate species was clade E, which is unique among the large-bodied Uluguru *Typoderus* by having elytral apices jointly rounded (Table 3, Fig. 2). Judging by morphology alone, Uluguru specimens herein forming clade K were suspected as representatives of perhaps a half dozen newly detected species (particularly the specimens so dissimilar among themselves as 2060, 2073, 2132 and 2155, the latter two genetically almost identical, Fig. 2). Recovery of the strongly supported clade K with morphologically most variable specimens (Fig. 2) is, therefore, the one of two most unexpected results of this study.

The second most unexpected result is the strongly supported genetic identity of clade H with respect to clade K. In other words, why the morphologically most similar specimens such as 3632 and 2171 detected in the same sample are consistently assigned to clades H and K, respectively? Each of these two clades has 100% statistical support in the concatenated dataset (and consistently recovered in all five other analyses) and they are rendered paraphyletic by *T. subfurcatus* (Fig. 2); although they are weakly supported as sisters in Fig. S3 and are strongly supported sisters in both analyses lacking the outgroup (Figs. 2 and S6). What are the evolutionary forces driving the extreme morphological diversity within clade K (Fig. 2) and, if the latter is indeed conspecific with the sympatric clade H, what is the reason for their strongly pronounced genetic identity?

With the data currently available, the most balanced evolutionally (and taxonomic) interpretation of clades H and K is to consider them as belonging to the same species with significant and independently driven genetic and morphological variability. The non-monophyly of this candidate species (Fig. 2) might perhaps be attributed to either the inadequately small dataset, or to the stochastic factors influenced by the outgroup selection. The latter hypothesis gains support from both temporal analyses, where in the absence of the *Lupangus* outgroup, both clades H and K form a strongly supported clade (Figs. 2, S6). Preferring the more conservative approach to taxonomy, only the more populous of these two clades is herein formally named (clade K), while clade H is given an interim informal numerical name (sp. 1808, Fig. 2), which later will perhaps be shown as synonymous with that of clade K.

4.3. New taxonomic acts

4.3.1. *Typoderus* Marshall, 1953: 104

Type species. *Typoderus machadoi* Marshall, 1953, by original designation.

Diagnosis. Presence of two zigzag-shaped longitudinal keels extending the entire length of the pronotum (Fig. 2) uniquely defines the *Lupangus* + *Typoderus* clade among all weevils. Longitudinal and perhaps homologous pronotal keels of the Typoderini genera *Pentaparopion* Morimoto, 1982 and *Styphloderes* Wollastone, 1873 are either straight (the former, Morimoto 1982: 106) or notably different in shape (the latter). Adults of *Lupangus* and *Typoderus* might be separated using characters given in Grebennikov (2017), together with an easy-to-observe difference in the rostrum orientation (fig. 34 therein; directed ventrad in *Lupangus* and anterad or at most anterio-ventrad in *Typoderus*), as well as presence (*Typoderus*, Fig. 4E,M,U) versus absence (*Lupangus*) of spines in the endophallus.

4.3.2. *Typoderus admetus* sp.n.
Fig. 4A–H

Diagnostic description. Holotype male (Fig. 4A–H), length between anterior edge of pronotum and elytral apex 7.0 mm, DNA data: Table 1. Aedeagus about 3 × as long as wide, with one sclerotized spine in endophallus (Fig. 4E–G). Unique combination of other morphological characters as in Table 3.

Material examined. ***Type material***: Holotype male (CNC): "TANZANIA, east slope southern Uluguru Mts., S07°07′20″ E037°38′37″, 18.xi.2010, 2058 m, sifting18, V.Grebennikov", "CNCCOLVG00002064". Paratypes (CNC): 26 specimens, as in Fig. 2.

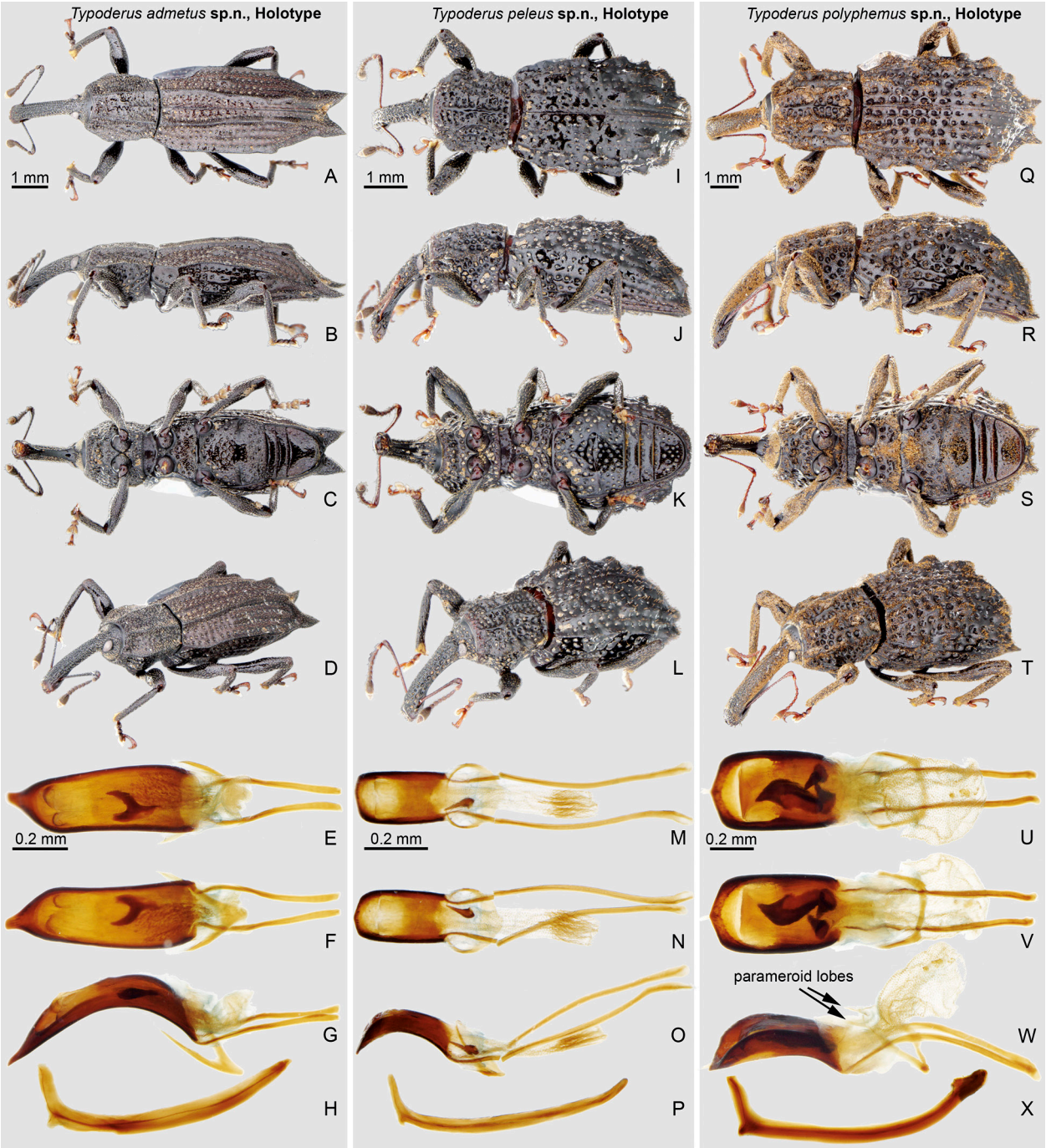

Fig. 4. Holotypes (all males) of three newly described Uluguru *Typoderus* species. **A–H**: *T. admetus* sp.n., **I–P**: *T. peleus* sp.n., **Q–X**: *T. polyphemus* sp.n. A–D, I–L, Q–T: habitus (A,I,Q: dorsal; B,J,R: lateral; C,K,S: ventral; D,L,T: fronto-latero-dorsal). E–H, M–P, U–X: genitalia (E,M,U: aedeagus dorsal; F,N,V: aedeagus ventral: G,O,W: aedeagus lateral; H,P,X: sternite 9).

Distribution. Known only from the Uluguru Mountains, Tanzania. Elevation: 1,569–2,408 m.

Etymology. Admetus, from ancient Greek mythology, one of the Argonauts, the host of Heracles and the husband of Aclestis; noun in apposition.

4.3.3. *Typoderus peleus* sp.n.
Fig. 4I–P

Diagnostic description. Holotype male (Fig. 4I–P), length between anterior edge of pronotum and elytral apex 5.9 mm, DNA data: Table 1. Aedeagus about 2 × as long as wide, with one sclerotized spine in endophallus (Fig. 4M–O). Unique combination of other morphological characters as in Table 3.

Material examined. ***Type material***: Holotype male (CNC): "TANZANIA, Uluguru Mts. at Bunduki vil., S07°00′15″ E37°37′50″, 24.xi.2010, 1848 m, sifting24, V.Grebennikov", "CNCCOLVG00 002130". Paratypes (CNC): 8 specimens, as in Fig. 2.

Distribution. Known from three localities in Tanzania: the Uluguru Mountains, Kimboza forest and Pugu Hills; respective elevations are 1,848 m, 237–271 m and 166 m.

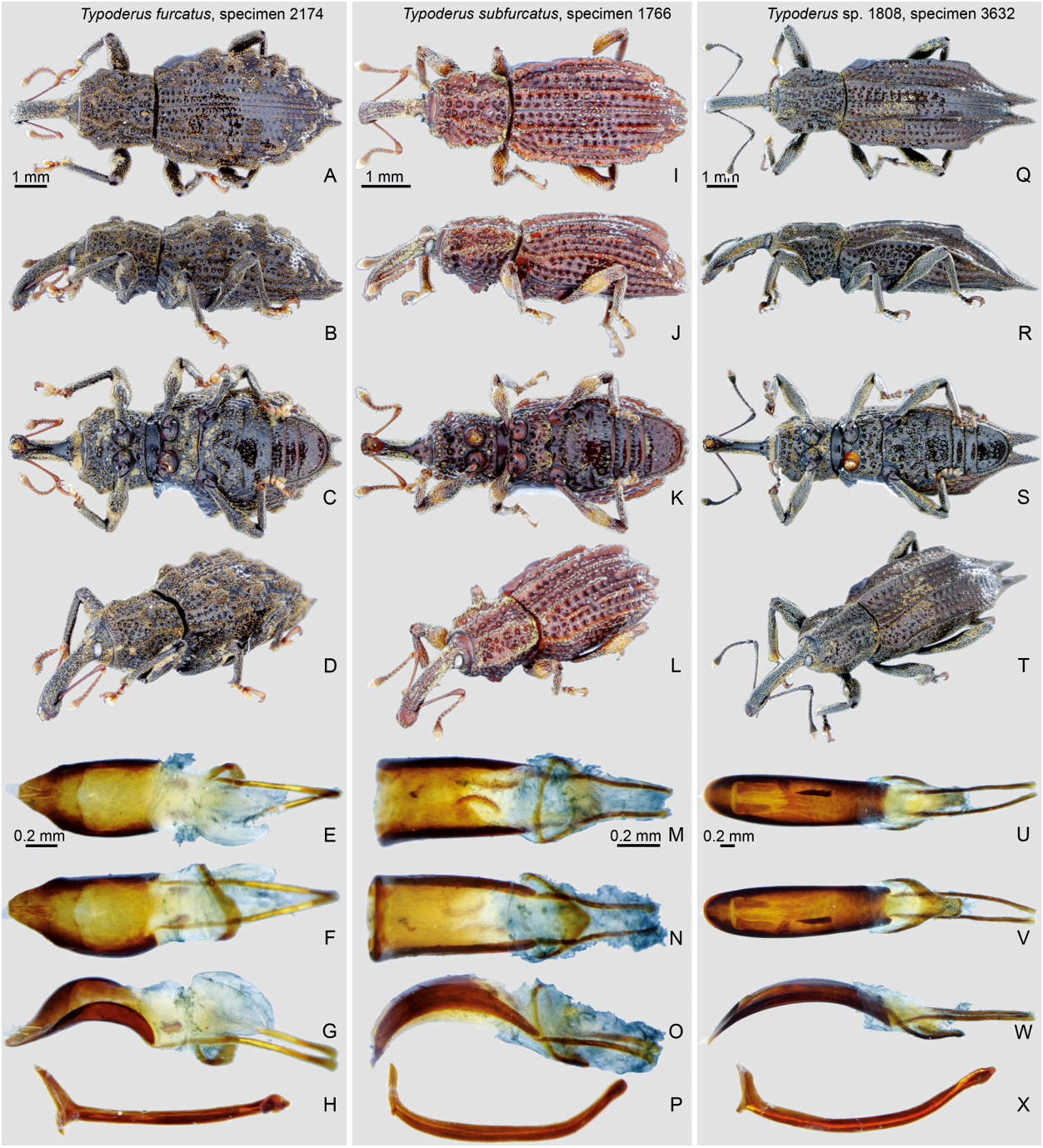

Fig. 5. Select male specimens of Uluguru *Typoderus* species. **A–H**: *T. furcatus*, **I–P**: *T. subfurcatus*, **Q–X**: *Typoderus* sp. 1808. A–D, I–L, Q–T: habitus (A,I,Q: dorsal; B,J,R: lateral; C,K,S: ventral; D,L,T: fronto-latero-dorsal). E–H, M–P, U–X: genitalia (E,M,U: aedeagus dorsal; F,N,V: aedeagus ventral: G,O,W: aedeagus lateral; H,P,X: sternite 9).

Etymology. Peleus, from ancient Greek mythology, one of the Argonauts, father of Achilles; noun in apposition.

4.3.4. *Typoderus polyphemus* sp.n.
Fig. 4Q–X

Diagnostic description. Holotype male (Fig. 4Q–X), length between anterior edge of pronotum and elytral apex 9.6 mm, DNA data: Table 1. Aedeagus about 2 × as long as wide, with three sclerotized spines in endophallus (Fig. 4E–G). Nearly unique combination of other morphological characters as in Table 3.

Remark. Small specimens of this species might be confused with larger specimens of *T. furcatus* (Table 3, Fig. 2); among them the new species is distinct by notably more parallel-sided (= not evenly rounded) pronotum and elytra in dorsal view (Fig. 2), as well as by having an abdominal pit. The most compelling evidence necessitating species status for these beetles is their sympatry with *T. furcatus* in Uluguru, which suggests different evolu-

tionary histories of both clades and lack of gene flow. This species also appears unique in having parameroid lobes (Fig. 4W, *sensu* Wanat 2007), even though only six *Typoderus* males were dissected (Figs. 4, 5).

Material examined. ***Type material***: Holotype male (CNC): "TANZANIA, Uluguru Mts. at Bunduki vil., S07°00′15″ E037°37′50″, 24.xi.2010, 1848 m, sifting24, V.Grebennikov", "CNCCOLVG00 002133". Paratypes (CNC): 2 specimens, as in Fig. 2.

Distribution. Known only from the Uluguru Mountains, Tanzania. Elevation: 1,569 – 1,848 m.

Etymology. Polyphemus, from ancient Greek mythology, one of the Cyclopes, the one blinded by the Odysseus' crew; noun in apposition.

4.4. Phylogeography of Uluguru *Typoderus*

The most notable phylogeographical signature of *Typoderus* in Tanzania is that all 70 herein analysed specimens are consistently grouped in 11 geographically and morphologically coherent clades (Fig. 2). Three non-endemic Uluguru *Typoderus* have conspecific monophyletic populations in either East Usambara (*T. furcatus*) or in the nearby Kimboza forest (Fig. 1D, *T. subfurcatus* and *T. peleus* sp.n.; the latter is also known from Pugu Hills). Reciprocal monophyly of the 11 clades is best interpreted as the standard signature of simple vicariance of a widespread ancestor (Heads 2014: 6). On the other hand, reported data offer no credible evidence of the founder (= chance; long distance) dispersal.

Lack of founder dispersal is particularly notable when comparing *Typoderus* fauna of Uluguru and Kimboza forest. Both forests are less than 18 km apart and lay in direct view of each other (Fig. 1D). Kimboza *Typoderus* consist of only two species, both of them found in Uluguru. Remarkably, Kimboza and Uluguru populations of each shared species are reciprocally monophyletic and the both most recent common ancestors are not younger than 5 MA (Fig. 3, but see below on uncertainty of time calibration). Even more remarkably, the Kimboza population of *T. peleus* sp.n. appears more closely related to that of the 10 times more distant Pugu Hills, than to those in the nearby Uluguru (Figs. 1, 2). These data strongly suggest that in spite of geographical proximity, the gene flow between Uluguru and Kimboza *Typoderus* was not much different, than that between Uluguru and about 10 – 15 times more distant Pugu Hills and East Usambara. The absence in Kimboza of three other Uluguru *Typoderus* species (*T. admetus* sp.n., *T. furcatus*, *T. polyphemus* sp.n.) further strengthen this conclusion (particularly that of *T. admetus* sp.n., which is the most frequently encountered).

Two among five nominal *Typoderus* known from Uluguru are endemic to this EAM forest: *T. admetus* sp.n. and *T. polyphemus* sp.n. Preliminary data from other EAM blocks suggest, however, that Uluguru might have not a single endemic *Typoderus* species, since morphologically and genetically similar beetles have been detected in at least Nguru and Udzungwa (Fig. 1B). Such results, if indeed correct, would suggest that the widely assumed single-block EAM endemism (Grebennikov 2017) might in at least some cases be attributed to either inadequate sampling, or taxonomic splitting, or both.

Table 3. Morphological characters and matrix for diagnostics of all six named *Typoderus* species known in Tanzania, three of which are herein described as new (excluding *Typoderus* sp. 1808, which is morphologically indistinguishable from, and perhaps conspecific with, *T. admetus* sp.n.). — **1** Body, distance between anterior edge of pronotum and elytral apex (continuous value in mm). — **2** Body, colour in dorsal view, reddish tint (character best studied in series containing mature and fully sclerotized specimens; beetles in nature are often covered by dense light-grey crust of solidified dust which should be soaked and brushed off to reveal body surface; compare cleaned specimen 2175 of *T. polyphemus* sp.n. in Fig. 2 with not cleaned specimen 2134): absent, body black (0); present, at least outside of pronotal and elytral discs (1). — **3** Antennae, number of antennomeres in funicle: five (5); seven (7). — **4** Elytra, shoulders, their angle in dorsal view: not (shoulders rounded) or weakly angulate (angle > 100° and not pointed anteriorly); (0); more strongly angulate (angle < 90° and pointed anteriorly) (1). — **5** Elytra, apices: jointly rounded or at most with a minor notch interrupting joint contour (0); separately rounded and each distinctly projecting posteriorly (1). — **6** Elytra, separately projecting apices, shape: continuously tapering, broad bases of left and right projections contiguous at elytral suture (0); nearly parallel-sided, bases of left and right projections distinctly separate by more than length of one projection (1). — **7** Abdomen, ventrite 2, central deep pit, ventral view: absent (0); present (1). — **8** Aedeagus, endophallus, number of spines: one (1); two (2); three (3). — **9** Aedeagus, ratio of maximal length to maximal width: two (2), three (3).

Species	1	2	3	4	5	6	7	8	9
T. admetus sp.n.	6.5–10.1	0	7	0	1	0	0	1	3
T. antennarius	3.3–3.8	1	5	1	0	n/a	0	?	?
T. furcatus	6.7–9.0	0	7	0	1	0&1	0	2	2
T. peleus sp.n.	5.9–7.3	0	7	0	0	n/a	0	1	2
T. polyphemus sp.n.	9.0–9.6	0	7	0	1	1	1	3	2
T. subfurcatus	3.2–5.6	1	7	0	0&1	1	0	2	2

4.5. Uncertainty in dating *Typoderus* evolution

No fossil is available for calibrating the *Typoderus* tree, while unlike the ages of volcanic islands (Papadopoulou et al. 2010), those of the island-type EAM forests are inadequately known and can't be used for clade calibration. The only available calibration method is to apply uniform nucleotide substitution rates established for the DNA barcode fragment in related organisms. These rates vary around 0.018 subs/s/Myr/l in beetles and among related arthropods. This approach contains a danger of great age overestimation, since for biologically most similar *Trigonopterus* weevils from the forest litter of the Oriental Region this rate might be at least four times greater (0.0793 subs/s/Myr/l, analysis 2 in Tänzler et al. 2016). This fast rate is in agreement with the hypothesis that molecular evolution in flightless beetles, especially

those inhabiting stable habitats such as EAM forests, might be highly accelerated (Mitterboeck & Adamowicz 2013). If indeed so, the absolute time values in Figs. 2 and S6 should be smaller by about the factor of four. Considering this uncertainty, little can be inferred from the recovered dates of *Typoderus* evolution (Figs. 2, S6), besides an observation that no dispersal/vicariance event took place during the Pleistocene (the last 2.61 MY) or, if faster rates are indeed correct, then within its last quarter (the last 0.6 MY).

4.6. "Rare" *Typoderus* in Uluguru

Three among five Uluguru *Typoderus* might be called "rare". *Typoderus furcatus* and *T. peleus* sp.n. (clades B and E, Fig. 2) are know from three and nine specimens, respectively, all detected in a single sifting sample (UL20 and UL17, respectively). Similarly rare is *T. polyphemus* sp.n., which is known from three specimens detected in two samples (UL17 and UL20; remarkably, these are the same species-rich samples mentioned above). Two remaining Uluguru species, *T. subfurcatus* and *T. admetus* sp.n. (the latter provisionally including *Typoderus* sp. 1808, which might perhaps be conspecific, see above), were detected in great numbers in nearly each among 22 samples (including the aforementioned samples UL17 and UL20). These results strongly suggest that the distribution of at least three *Typoderus* species across the Uluguru forest is not random and, therefore, additional species might have been overlooked.

4.7. Phylogeographic potential of *Typoderus* and direction for future research

The herein documented evolution of the weevil genus *Typoderus* within the geographical context of EAM and nearby forests strongly suggests that the genus is phylogeographically informative. This is not unexpected since nearly each consistently sampled and thoroughly analysed shallow and specious clade of flightless weevils offers phylogeographical insights (see Grebennikov 2017 for a review). *Typoderus* weevils in this respect seem particularly informative, since they possess at least one more and still untapped source of discrete information: comparative morphology of their diverse male genitalia (including such a discrete, non-adaptive and easy to observe character as the number of internal spines, Figs. 4E,M,U, 5E,M,U).

5. Acknowledgements

Ignacio Ribera (Barcelona, Spain) advised on the logic and technicalities of DNA analysis. Bradley Sinclair (Ottawa, Canada), Ole Seehausen (Bern, Switzerland) and Peter Hlaváč (Prague, Czech Republic) commented on an earlier version of this paper prior to its submission.

6. References

Andújar C., Serrano J., Gómez-Zurita J. 2012. Winding up the molecular clock in the genus *Carabus* (Coleoptera: Carabidae): assessment of methodological decisions on rate and node age estimation. – BMC Evolutionary Biology **12**(40): 16 pp. doi: 10.1186/1471-2148-12-40

Barley A., White J., Diesmos A.C., Brown R.M. 2013. The challenge of species delimitation at the extremes: diversification without morphological change in Philippine sun skinks. – Evolution **67**: 3556–3572. doi: 10.1111/evo.12219

Bray T.C., Bocak L. 2016. Slowly dispersing neotenic beetles can speciate on a penny coin and generate space-limited diversity in the tropical mountains. – Scientific Reports **33579**: 1–9. doi: 10.1038/srep33579

deMenocal P.B. 2004. African climate change and faunal evolution during the Pliocene–Pleistocene. – Earth and Planetary Science Letters **220**: 3–24.

de Queiroz K. 2007. Species concepts and species delimitation. – Systematic Biology **56**: 879–886. doi: 10.1080/10635150701701083

Drummond A.J., Suchard M.A., Xie D., Rambaut A. 2012. Bayesian phylogenetics with BEAUti and the BEAST 1.7. – Molecular Biology and Evolution **29**: 1969–1973. doi: 10.1093/molbev/mss075

Faria C.M.A., Machado A., Amorim I.R., Gage M.J.G., Borges P.A.V., Emerson B.C. 2016. Evidence for multiple founding lineages and genetic admixture in the evolution of species within an oceanic island weevil (Coleoptera, Curculionidae) super-radiation. – Journal of Biogeography **43**: 178–191. doi: 10.1111/jbi.12606

Felsenstein J. 1985. Confidence limits on phylogenies: an approach using the bootstrap. – Evolution **39**: 783–791. doi: 10.2307/2408678

Finch J., Leng M.J., Marchant R. 2009. Late Quaternary vegetation dynamics in a biodiversity hotspot, the Uluguru. – Quaternary Research **72**: 111–122. doi: 10.1016/j.yqres.2009.02.005

Futahashi R., Shirataki H., Narita T., Mita K., Fujiwara H. 2012. Comprehensive microarray-based analysis for stage-specific larval camouflage patternassociated genes in the swallowtail butterfly, *Papilio xuthus*. – BMC Biology **10**(46): 21 pp. doi: 10.1186/1741-7007-10-46

Grebennikov V.V. 2014a. DNA barcode and phylogeography of six new high altitude wingless *Niphadomimus* (Coleoptera: Curculionidae: Molytinae) from Southwest China. – Zootaxa **3838**: 151–173. doi: 10.11646/zootaxa.3838.2.1

Grebennikov V.V. 2014b. *Morimotodes*, a new genus for two minute wingless litter species from southwest China and Taiwan with an illustrated overview of Molytina and Plinthina genera (Coleoptera: Curculionidae: Molytini). – Bonn Zoological Bulletin **63**: 123–147.

Grebennikov V.V. 2015a. Wingless *Paocryptorrhinus* (Coleoptera: Curculionidae) rediscovered in Tanzania: synonymy, four new species and a mtDNA phylogeography. – Bonn Zoological Bulletin **64**: 1–15.

Grebennikov V.V. 2015b. Neglected *Trichalophus* (Coleoptera: Curculionidae): DNA barcode and phylogeography of high altitude flightless weevils rediscovered in Southwest China. – Bonn Zoological Bulletin **64**: 59–76.

Grebennikov V.V. 2017. Phylogeography and sister group of *Lupangus*, a new genus for three new flightless allopatric forest litter weevils endemic to the Eastern Arc Mountains, Tanzania (Coleoptera: Curculionidae, Molytinae). – Fragmenta Entomologica **49**: 37–55.

Grebennikov V.V. 2018a. Re-defined *Aparopionella* from Afrotropical forest floors comprises 20 poorly known nominal species (Coleoptera, Curculionidae, Molytinae). – Entomologische Blätter und Coleoptera **114**: 219–231.

Grebennikov V.V. 2018b. Phylogenetically problematic *Aater cangshanensis* gen. et sp. nov. from Southwest China suggests multi-

ple origins of prosternal canal in Molytinae weevils (Coleoptera: Curculionidae). – Fragmenta Entomologica **50**: 103–110.

Hamilton A.C., Taylor D. 1991. History of climate and forests in tropical Africa during the last 8 million years. – Climatic Change **19**: 65–78.

Hebert P.D.N., Cywinska A., Ball S.L., DeWaard J.R. 2003a. Biological identifications through DNA barcodes. – Proceedings of the Royal Society B: Biological Sciences **270**: 313–321. doi: 10.1098/rspb.2002.2218

Hebert P.D.N., Ratnasingham S., DeWaard J.R. 2003b. Barcoding animal life: cytochrome c oxidase subunit 1 divergences among closely related species. – Proceedings of the Royal Society B: Biological Sciences **270**: 96–99. doi: 10.1098/rsbl.2003.0025

Heads M. 2014. Biogeography of Australasia. A Molecular Analysis. – Cambridge University Press, Cambridge. 503 pp.

Ivanova N.V., DeWaard J.R., Hebert P.D.N. 2006. An inexpensive, automation-friendly protocol for recovering high-quality DNA. – Molecular Ecology Notes **6**: 998–1002. doi: 10.1111/j.1471-8286.2006.01428.x

Katoh K., Misawa K., Kuma K., Miyata T. 2002. MAFFT: a novel method for rapid multiple sequence alignment based on fast Fourier transform. – Nucleic Acids Research **30**: 3059–3066. doi: 10.1093/nar/gkf436

Katoh K., Toh H. 2008a. Recent developments in the MAFFT multiple sequence alignment program. – Briefings in Bioinformatics **9**: 286–298. doi: 10.1093/bib/bbn013

Katoh K., Toh H. 2008b. Improved accuracy of multiple ncRNA alignment by incorporating structural information into a MAFFT-based framework. – BMC Bioinformatics **9**: 212. doi: 10.1186/1471-2105-9-212

Kumar S., Stecher G., Tamura K. 2016. MEGA7: Molecular evolutionary genetics analysis Version 7.0 for bigger datasets. – Molecular Biology and Evolution **33**: 1870–1874. doi: 10.1093/molbev/msw054

Lovett J.C., Wasser S.K. (eds) 1993. Biogeography and Ecology of the Rain Forests of Eastern Africa. – Cambridge University Press, Cambridge. 341 pp.

Lyal C.H. 2014. 3.7.7 Molytinae Schoenherr, 1823. Pp. 434–451 in: Leschen R.A.B., Beutel R.G. (eds), Handbook of Zoology, Arthropoda: Insecta: Coleoptera. Volume 3: Morphology and Systematics (Phytophaga). – Walter de Gruyter, Berlin. 674 pp.

Maddison W.P., Maddison D.R. 2011. Mesquite: A Modular System for Evolutionary Analysis. Version 3.04. – URL < https://www.mesquiteproject.org/ > [accessed 07 September 2018]

Maley J. 1996. The African rain forest – main characteristics of changes in vegetation and climate from the Upper Cretaceous to the Quaternary. In Alexander I.J., Swaine M.D., Watling R. (eds), Essays on the Ecology of the Guinea-Congo rain forest. – Proceedings of the Royal Society of Edinburgh **104B**: 31–73.

Marshall G.A.K. 1953. On a collection of Curculionidae (Coleoptera) from Angola. – Publicaçôes Culturais da Companhia de Diamantes de Angola **16**: 98–119.

Marshall G.A.K. 1955. Contributions à l'étude de la faune entomologique du Ruanda-Urundi (Mission P. Basilewsky 1953). LXVI. Coleoptera Curculionidae. – Annales du Musée Royal du Congo Belge, Série in 8° **40**: 240–295.

Marshall G.A.K. 1957. On the genus *Typoderus* Mshl. (Coleoptera Curculionidae). – Revue de Zoologie et de Botanique Africaines **55**: 389–395.

Measey G.J., Tolley K.A. 2011. Sequential fragmentation of Pleistocene forests in an East Africa biodiversity hotspot: chameleons as a model to track forest history. – PLoS ONE **6**(10): e26606, 9 pp. doi: 10.1371/journal.pone.0026606

Miller M.A., Pfeiffer W., Schwartz T. 2010. "Creating the CIPRES Science Gateway for inference of large phylogenetic trees" in Proceedings of the Gateway Computing Environments Workshop (GCE), 14 Nov. 2010, New Orleans, LA, pp. 1–8.

Mitterboeck T.F., Adamowicz S.J. 2013. Flight loss linked to faster molecular evolution in insects. – Proceedings of the Royal Society B **280**: 20131128, 8 pp. doi: 10.1098/rspb.2013.1128

Morimoto K. 1982. The family Curculionidae of Japan. I. Subfamily Hylobiinae. – Esakia **19**: 51–121.

Mumbi C.T., Marchant R., Hooghiemstra H., Wooller M.J. 2008. Late Quaternary vegetation reconstruction from the Eastern Arc Mountains, Tanzania. – Quaternary Research **69**: 326–341. doi: 10.1016/j.yqres.2007.10.012

Papadopoulou A., Anastasiou I., Vogler A.P. 2010. Revisiting the insect mitochondrial molecular clock: the mid-aegean trench calibration. – Molecular Biology and Evolution **27**: 1659–1672. doi: 10.1093/molbev/msq051

Rambaut A. 2014. FigTree, Version 1.4. – URL < http://tree.bio.ed.ac.uk/software/figtree/ > [accessed 12 March 2018].

Ratnasingham S., Hebert P.D.N. 2007. BOLD: The Barcode of Life Data System (http://www. barcodinglife. org). – Molecular Ecology Notes **7**: 355–364. doi: 10.1111/j.1471-8286.2006.01678.x

Ratnasingham S., Hebert P.D.N. 2013. A DNA-based registry for all animal species: the Barcode Index Number (BIN) system. – PLoS ONE **8**: e66213, 16 pp. doi: 10.1371/journal.pone.0066213

Shorthouse D.P. 2010. SimpleMappr, an online tool to produce publication-quality point maps. – URL < http://www.simplemappr.net > [accessed 12 March 2018].

Stamatakis A., Hoover P., Rougemont J. 2008. A rapid bootstrap algorithm for the RAxML web servers. – Systematic Biology **57**: 758–771. doi: 10.1080/10635150802429642

Tänzler R., Van Dam M.H., Toussaint E.F.A., Suhardjono Y.R., Balke M., Riedel A. 2016. Macroevolution of hyper diverse flightless beetles reflects the complex geological history of the Sunda Arc. – Scientific Reports **6**: 18793, 12 pp. doi: 10.1038/srep18793

Tänzler R., Sagata K., Surbakti S., Balke M., Riedel A. 2012. DNA Barcoding for community ecology – how to tackle a hyperdiverse, mostly undescribed Melanesian fauna. – PLoS ONE **7**: e28832, 11 pp. doi: 10.1371/journal.pone.0028832

Toussaint E.F.A., Tänzler R., Balke M., Riedel A. 2017. Transoceanic origin of microendemic and flightless New Caledonian weevils. – Royal Society Open Science **4**: 160546, 11 pp. doi: 10.1098/rsos.160546

Voss E. 1962. Attelabidae, Apionidae, Curculionidae (Coleoptera Rhynchophora). – Exploration du Parc National de l'Upemba Mission G F de Witte. Fascicule 44. – Institut des Parcs Nationaux du Congo Belge, Bruxelles, 380 pp.

Voss E. 1965. Mission zoologique de l'I.R.S.A.C. en Afrique Orientale (P. Basilewsky et N. Leleup, 1957). Résultats scientifiques. Cinquième partie. Coleoptera Curculionidae II (Schluss). – Annales du Musée Royal de l'Afrique Centrale, Tervuren (Série in 8°, Zoologie) **138**: 293–377.

Wanat M. 2007. Alignment and homology of male terminalia in Curculionoidea and other Coleoptera. – Invertebrate Systematics **21**: 147–171. doi: 10.1071/IS05055

Ward P. 2011. Integrating molecular phylogenetic results into ant taxonomy (Hymenoptera: Formicidae). – Myrmecological News **15**: 21–29.

Zahiri R., Lafontaine J.D., Schmidt C.C., Zakharov E.V., Hebert P.D.N. 2017. Probing planetary biodiversity with DNA barcodes: the Noctuoidea of North America. – PloS one **12**: e0178548, 18 pp. doi: 10.1371/journal.pone.0178548

Zhang G., Basharat U., Matzke N., Franz N.M. 2017. Model selection in statistical historical biogeography of Neotropical insects – the *Exophthalmus* genus complex (Curculionidae: Entiminae). – Molecular Phylogenetics and Evolution **109**: 226–239. doi: 10.1016/j.ympev.2016.12.039

Electronic Supplement File

at http://www.senckenberg.de/arthropod-systematics

File 1: grebennikov-typoderusweevils-asp2019-electronicsupplement-1.pdf. — **Table S1.** List of sampled localities. EAM: Eastern Arc Mountains, LF: lowland forests, VH: volcanic highlands. — **Table S2.** List of used primers . — **Fig. S1.** Images of 105 DNA barcoded *Typoderus* from Uluguru (including one larva and one pupa). — **Fig. S2.** Neighbour Joining clustering of DNA barcodes of 105 Uluguru *Typoderus*. Topological clustering was done using the online BOLD tree-building engine utilizing pairwise distance and the NJ algorithm. — **Fig. S3.** Maximum Likelihood inference phylogram of *Typoderus* weevils generated using COI matrix with 71 terminals and 658 bp; terminal labels as in Fig. 2. — **Fig. S4.** Maximum Likelihood inference phylogram of *Typoderus* weevils generated using ITS2 matrix with 68 terminals and 772 bp; terminal labels as in Fig. 2. — **Fig. S5.** Maximum Likelihood inference phylogram of *Typoderus* weevils generated using 28S matrix with 69 terminals and 595 bp; terminal labels as in Fig. 2. — **Fig. S6.** Ultrametric time tree of 70 *Typoderus* obtained with BEAST using 0.018 subs/s/Myr/l rates for COI-5'. Terminal labels as in Fig. 2. Numbers on scale are million years before present. Node bars represent 95% confidence interval. — DOI: 10.26049/ASP77-2-2019-04/1

Zoobank Registrations

at http://zoobank.org

Present article: http://zoobank.org/urn:lsid:zoobank.org:pub:F65F997D-ECF1-48CC-BB68-A73204DC39A8

Typoderus admetus* Grebennikov, 2019*: http://zoobank.org/urn:lsid:zoobank.org:act:8816B11E-D1CC-4083-A5FB-BBE862D2EEA4

***Typoderus peleus* Grebennikov, 2019:** http://zoobank.org/urn:lsid:zoobank.org:act:4421542B-0430-45E6-AD0E-6F3B959418AA

***Typoderus polyphemus* Grebennikov, 2019:** http://zoobank.org/urn:lsid:zoobank.org:act:7750C57B-BE0E-4FAF-A6E1-744A92907F1C